

Defective One- or Two-electron Reduction of the Anticancer Anthracycline Epirubicin in Human Heart

RELATIVE IMPORTANCE OF VESICULAR SEQUESTRATION AND IMPAIRED EFFICIENCY OF ELECTRON ADDITION*

Received for publication, July 29, 2005, and in revised form, December 12, 2005. Published, JBC Papers in Press, January 19, 2006, DOI 10.1074/jbc.M508343200

Emanuela Salvatorelli^{†1}, Simone Guarnieri^{‡1}, Pierantonio Menna^{‡1}, Giovanni Liberi[§], Antonio M. Calafiore^{¶2}, Maria A. Marigliò[‡], Alvaro Mordente^{||}, Luca Gianni^{**}, and Giorgio Minotti^{‡3}

From the [†]Center of Excellence on Aging and [§]Department of Cardiac Surgery, G. d'Annunzio University School of Medicine, 66013 Chieti, [¶]Unit of Cardiac Surgery, European Hospital, 00148 Rome, ^{||}Institute of Biochemistry and Clinical Biochemistry, Catholic University School of Medicine, 00168 Rome, and ^{**}Unit of Medical Oncology, Istituto Nazionale Tumori, 20133 Milan, Italy

One-electron quinone reduction and two-electron carbonyl reduction convert the anticancer anthracycline doxorubicin to reactive oxygen species (ROS) or a secondary alcohol metabolite that contributes to inducing a severe form of cardiotoxicity. The closely related analogue epirubicin induces less cardiotoxicity, but the determinants of its different behavior have not been elucidated. We developed a translational model of the human heart and characterized whether epirubicin exhibited a defective conversion to ROS and secondary alcohol metabolites. Small myocardial samples from cardiac surgery patients were reconstituted in plasma that contained clinically relevant concentrations of doxorubicin or epirubicin. In this model only doxorubicin formed ROS, as detected by fluorescent probes or aconitase inactivation. Experiments with cell-free systems and confocal laser scanning microscopy studies of H9c2 cardiomyocytes suggested that epirubicin could not form ROS because of its protonation-dependent sequestration in cytoplasmic acidic organelles and the consequent limited localization to mitochondrial one-electron quinone reductases. Accordingly, blocking the protonation-sequestration mechanism with the vacuolar H⁺-ATPase inhibitor bafilomycin A1 relocalized epirubicin to mitochondria and increased its conversion to ROS in human myocardial samples. Epirubicin also formed ~60% less alcohol metabolites than doxorubicin, but this was caused primarily by its higher K_m and lower V_{max} values for two-electron carbonyl reduction by aldo/ketoreductases of human cardiac cytosol. Thus, vesicular sequestration and impaired efficiency of electron addition have separate roles in determining a defective bioactivation of epirubicin to ROS or secondary alcohol metabolites in the human heart. These results uncover the molecular determinants of the reduced cardiotoxicity of epirubicin and serve mechanism-based guidelines to improving antitumor therapies.

The anthracyclines doxorubicin (DOX)⁴ and epirubicin (EPI) are topoisomerase II inhibitors that exhibit activity in breast cancer and

many other tumors (1). These drugs are composed of an aglycone and a sugar. The aglycone (doxorubicinone) consists of a tetracyclic ring with adjacent quinone-hydroquinone moieties and a short side chain with a carbonyl group; the sugar (daunosamine) is an amino-substituted trideoxy fucosyl moiety. Epirubicin differs from DOX in an axial-to-equatorial epimerization of the hydroxyl group at C-4' in daunosamine (Fig. 1). This minor difference renders EPI a much better substrate than DOX for human liver UDP-glucuronosyltransferase 2B7 and consequently facilitates the formation of glucuronides that are excreted in bile and urine (2). Improved glucuronidation and body clearance alter the dose-related antiproliferative activity of EPI, as shown by the fact that the dose of EPI equimyelotoxic to 1 mg of DOX is 1.5 mg (3).

A major obstacle to the clinical use of anthracyclines pertains to the development of cardiomyopathy and congestive heart failure upon chronic administration. Of note, the dose of EPI equicardiotoxic to 1 mg of DOX has been approximated to 1.8 mg for cardiac symptoms and 2.2 mg for injury on endomyocardial biopsies (3, 4). Thus, EPI causes cardiotoxicity at doses higher than equimyelotoxic to DOX, as if improved glucuronidation and systemic elimination were not the only factors that diminished its noxious interactions with cardiomyocytes. Uncovering the molecular determinant(s) that render EPI intrinsically less cardiotoxic than DOX would be of conceptual value in many settings.

Anthracycline-induced cardiotoxicity is a complex multifactorial process. The current thinking is that anthracyclines are toxic *per se* but gain further toxicity upon conversion to reactive oxygen species (ROS), like superoxide anion (O₂⁻) and its dismutation product hydrogen peroxide (H₂O₂). These species are formed through an enzymatic one-electron reduction of the quinone moiety, a process yielding a semiquinone that regenerates its parent quinone by oxidizing with oxygen (Fig. 1). Because of the lower levels of O₂⁻ and H₂O₂-detoxifying enzymes in cardiomyocytes as compared with other cell types, ROS amplify the cardiotoxicity of anthracyclines through oxidative stress, disruption of the cardiac-specific gene expression program, mitochondrial dysfunction, and apoptosis (reviewed in Refs. 1 and 5–7). Anthracycline semiquinones can also disproportionate and rearrange to 7-deoxydoxorubicinolone through a concomitant reductive cleavage of the glycosidic bond with daunosamine and reduction of the side chain carbonyl group (Fig. 1). 7-Deoxydoxorubicinolone therefore serves as a biochemical marker to probe a one-electron redox cycling of anthracyclines in biologic systems (8).

* This work was supported by Associazione Italiana Ricerca sul Cancro, Ministero dell'Università e Ricerca Scientifica e Tecnologica (MIUR), Cofin 2004, FIRB RBNE 014HJ3-002, and Center of Excellence on Aging at the University of Chieti. The costs of publication of this article were defrayed in part by the payment of page charges. This article must therefore be hereby marked "advertisement" in accordance with 18 U.S.C. Section 1734 solely to indicate this fact.

[†] These authors contributed equally to this work.

[‡] Present address: Department of Cardiac Surgery, University of Catania School of Medicine, 95124 Catania, Italy.

[§] To whom correspondence should be addressed: G. d'Annunzio University School of Medicine, Ce.S.I., Rm. 412, Via dei Vestini, 66013 Chieti, Italy. Tel.: 39-0871-541391; Fax: 39-0871-541480, E-mail: gminotti@unich.it.

⁴ The abbreviations used are: DOX, doxorubicin; EPI, epirubicin; ROS, reactive oxygen

species; O₂⁻, superoxide anion; H₂O₂, hydrogen peroxide; DOXOL, doxorubicinol; EPIOL, epirubicinol; DCFH-(DA), dichlorofluorescein (diacetate); DCF, dichlorofluorescein; AUC, area under the curve; Amplex Red reagent, 10-acetyl-3,7-dihydroxyphenoxazine; HPLC, high pressure liquid chromatography; NES, normal external solution.

Anthracyclines may gain toxicity also after a two-electron reduction of the side chain carbonyl group and formation of a secondary alcohol metabolite (Fig. 1). The latter contributes to down-regulating cardiac-specific genes (9) and inactivates calcium-handling proteins (10–12). Secondary alcohol metabolites may also act in concert with ROS and perturb the function of cytoplasmic aconitase/iron regulatory protein-1, an important regulator of iron homeostasis and redox balance in the cell (1, 13, 14). Although the actual weight of one mechanism or another remains a matter of some debate (1, 6, 7, 15), studies with laboratory animals showed that overexpression of ROS-detoxifying enzymes or genetic deletion of alcohol metabolite-producing enzymes always mitigated or delayed cardiotoxicity induced by DOX (16, 17).

We considered that a reduced level of formation of ROS and/or secondary alcohol metabolites would attenuate the effects of EPI in the heart, thus explaining how EPI causes cardiotoxicity at doses higher than equimyelotoxic to DOX. In examining this possibility, several important factors need to be taken into account. For example, ROS formation in anthracycline-treated cells was often shown to reflect acute damage and nonspecific metabolic perturbances rather than a specific capability of cardiomyocytes to promote a one-electron quinone reduction of these drugs (18). Moreover, anthracycline secondary alcohol metabolites are formed by enzymes that exhibit variable levels of expression in humans *versus* laboratory animals or in a given animal species and strain *versus* another (19, 20); hence, the results obtained with animal models do not allow general conclusions on the level of formation of secondary alcohol metabolites in humans. Finally, the conversion of anthracyclines to ROS and secondary alcohol metabolite may depend not only on their inherent susceptibility to the action of one- or two-electron reductases but also on their different localization to pertinent subcellular compartments. To meet these concerns and obtain molecular correlates to clinical findings, we characterized the distribution and reductive bioactivation of DOX and EPI in a properly designed translational model of human heart.

EXPERIMENTAL PROCEDURES

Chemicals—Doxorubicin, EPI, secondary alcohol metabolites (doxorubicinol/DOXOL and epirubicinol/EPIOL), 7-deoxydoxorubicinone, and 7-deoxydoxorubicinolone were kindly provided by Dr. Antonino Suarato (Nerviano Medical Sciences, Milan, Italy). Dichlorofluorescein diacetate (DCFH-DA), dichlorofluorescein (DCF), Mito Tracker Deep Red 633, Lyso Tracker Green DND-26, Amplex Red reagent (10-acetyl-3,7-dihydroxyphenoxazine), and resorufin (sodium salt) were purchased from Molecular Probes (Eugene, OR). Free DCFH was prepared by alkaline hydrolysis of DCFH-DA (21). Tolrestat was from Wyeth Ayerst Research (Princeton, NJ). Bafilomycin (type A1), horseradish peroxidase (type VI), and all other chemicals were from Sigma.

Assays for Anthracycline Metabolism in Human Myocardial Strips—Small myocardial samples were obtained from 60 male and female patients (68 ± 5 years) undergoing aortocoronary bypass grafting. All specimens were derived from the lateral aspect of excluded right atrium and were routinely disposed of by the surgeons during cannulation procedures for cardiopulmonary bypass; therefore, the patients were not subjected to any unjustified loss of tissue (22). Sampling procedures were in compliance with guidelines of the Institutional Ethical Committee, and written informed consent was obtained from all patients.

Thin strips (<0.1 g, ~ 10 mm long, and ~ 2 mm wide) were carefully dissected free of fat or grossly visible foreign tissues and washed extensively in ice-cold 0.3 M NaCl. Unless otherwise indicated, the strips were reconstituted in 2 ml of fresh human plasma in the absence or presence of 1 or 10 μ M anthracyclines. After 4 h of incubation at 37 °C in a

Dubnoff metabolic bath under an air atmosphere, the strips were washed in ice-cold 0.3 M NaCl, homogenized in a minimum volume of the same medium, and centrifuged for 90 min at $105,000 \times g$ to separate a soluble and a whole membrane fraction. The two fractions were extracted separately with a 4-fold volume of (1:1) $\text{CHCl}_3/\text{CH}_3\text{OH}$; the organic phases were combined, and 20 μ l were analyzed by reversed phase HPLC on an HP Zorbax CN column (250×4.6 mm, 5 μ m; Hewlett Packard Co., Palo Alto, CA) operated at 25 °C. Extracts of DOX-treated samples were eluted at the flow rate of 1.5 ml/min with a 15-min linear gradient from 50 mM NaH_2PO_4 to CH_3CN , 25 mM NaH_2PO_4 , pH 4.0. Retention times (R_t) were 10.9, 12.1, and 13.9 min for DOXOL, DOX, and 7-deoxydoxorubicinone, respectively. Extracts of EPI-treated samples were eluted isocratically with CH_3CN , 25 mM NaH_2PO_4 at the flow rate of 1.5 ml/min; R_t were 5.5, 7.5, and 9 min for EPIOL, EPI, and 7-deoxydoxorubicinone, respectively. 7-Deoxydoxorubicinolone was separated by chromatography on a Nucleosil C-18 column (100×4.6 mm, 5 μ m/Supelco, Bellefonte, PA), operated at 25 °C, and eluted with a 15-min linear gradient from 50 mM NaH_2PO_4 to CH_3CN , 25 mM NaH_2PO_4 at the flow rate of 1 ml/min. Retention time was 14 min. Anthracyclines were detected fluorimetrically (excitation at 480 nm/emission at 560 nm) and quantified against appropriate standard curves. Unless otherwise indicated, all values were expressed as nmol/g (wet weight).

Intramyocardial H_2O_2 Assay—We used a modification of the DCFH-DA method. DCFH-DA crosses the plasma membrane and releases DCFH after deacetylation by cellular esterases; in the presence of ROS, DCFH eventually oxidizes to form the green fluorescent DCF (21, 23). Myocardial strips were loaded with 50 μ M DCFH-DA in 4 ml of 50 mM phosphate buffer, 123 mM NaCl, 5.6 mM glucose, pH 7.4. After 1 h of incubation in the dark, the strips were washed with 0.3 M NaCl and reconstituted in human plasma in the absence or presence of DOX or EPI, as described above. Next, the strips were homogenized in 2 ml of ice-cold 123 mM NaCl that was added with the antioxidant 4-hydroxytempol (1 mM) to prevent further oxidation of DCFH to DCF during tissue homogenization. Soluble and membrane fractions were extracted with 2 volumes of (1:1) $\text{CH}_3\text{OH}-\text{CHCl}_3$, and 25 μ l of the upper phase were analyzed by HPLC using a Nucleosil C-18 column (100×4.6 mm, 5 μ m), operated at 25 °C. Samples were eluted at the flow rate of 1 ml/min with a 15-min linear gradient from 50 mM NaH_2PO_4 to CH_3CN , 25 mM NaH_2PO_4 , pH 4.0. The fluorescent peak of DCF (excitation at 488 nm/emission at 525 nm) was identified by co-chromatography with an authentic standard ($R_t = 18.3$ min), and its area under the curve (AUC) in membrane or soluble fractions was corrected for the corresponding AUC in strips extracted immediately after loading with DCFH-DA; the differences indicated the net level of DCF formation during 4 h of incubation of strips in plasma. To quantify H_2O_2 formation *versus* DCF fluorescence, we titrated myocardial strips with known amounts of H_2O_2 . Briefly, myocardial strips were loaded with DCFH-DA, washed, reconstituted in 4 ml of 50 mM phosphate buffer, 123 mM NaCl, 5.6 mM glucose, pH 7.4, and exposed for 15 min to 0.1, 1, 5, or 10 μ M H_2O_2 . At the end of treatments, the strips were washed and reconstituted in plasma for an additional 30 min at 37 °C. The total AUC of DCF in these samples (membrane fraction + soluble fraction) was corrected for that of strips extracted immediately after loading with DCFH-DA. The net differences correlated linearly with the concentrations of H_2O_2 delivered to the strips ($r = 0.80$, $p < 0.001$), and were quantified against a standard curve of 5 nM to 2.5 μ M authentic DCF ($r = 0.98$, $p < 0.0001$). On the basis of this procedure, we approximated that 1 nmol of H_2O_2 caused the formation of 0.43 ± 0.07 nmol of DCF/g of human myocardium ($n = 12$); this stoichiometry was routinely adopted to

Epirubicin and Mechanisms of Anthracycline Cardiotoxicity

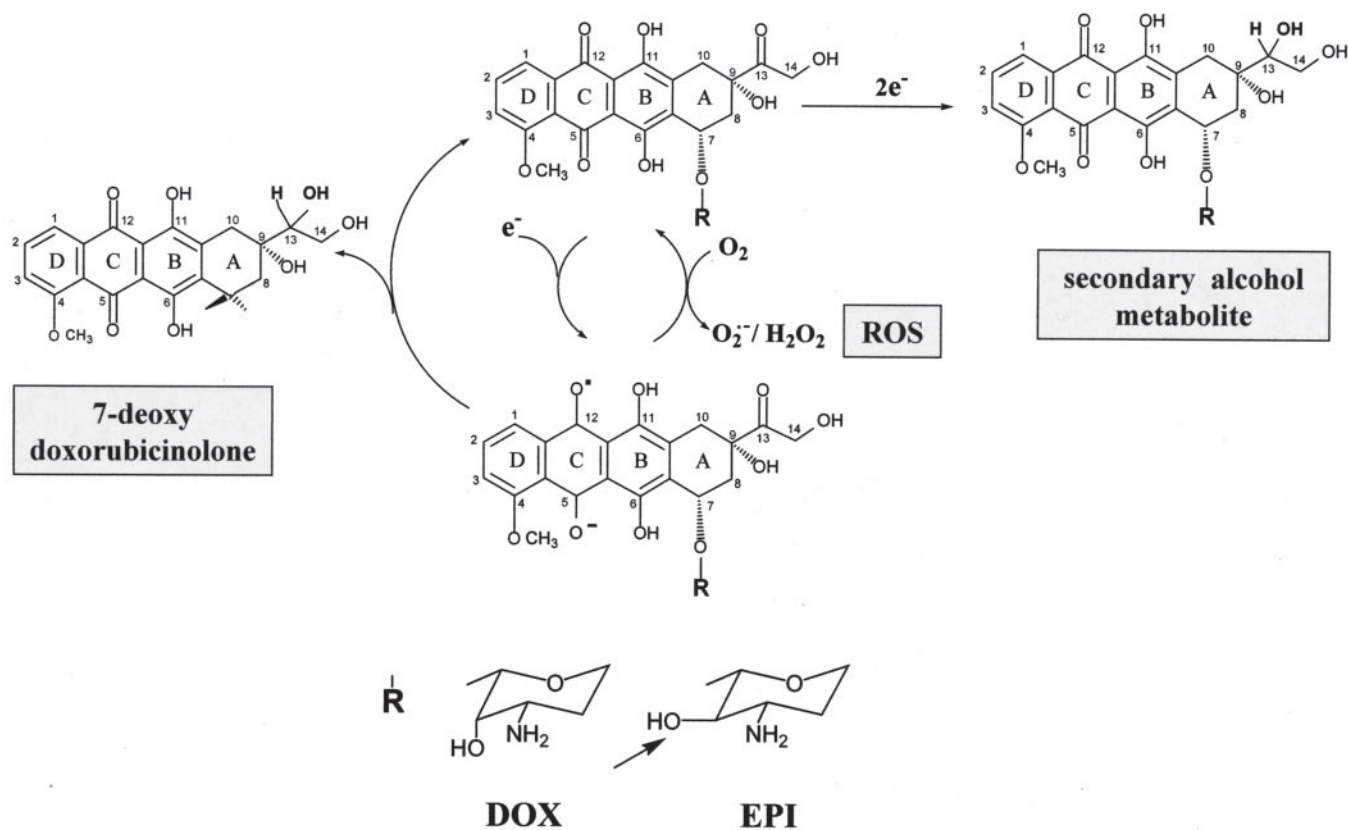


FIGURE 1. **Structures and reductive metabolism of DOX and EPI.** Doxorubicin and EPI share a tetracyclic ring, a carbonyl-containing side chain, and an amino sugar called daunosamine (*R*). EPI differs from DOX in an axial-to-equatorial epimerization of the hydroxyl group at C-4' in daunosamine (indicated by the arrow). This figure also shows one- or two-electron reductive metabolism of anthracyclines; one-electron reduction of the quinone moiety in ring C is accompanied by formation of ROS and 7-deoxydoxorubicinolone, whereas two-electron reduction of the side chain carbonyl group yields a secondary alcohol metabolite.

quantify basal or anthracycline-induced H_2O_2 formation in myocardial strips.

Extracellular H_2O_2 Assay—The Amplex Red reagent (10-acetyl-3,7-dihydroxyphenoxazine) enters the cells poorly, but in the presence of extracellular H_2O_2 and horseradish peroxidase it oxidizes to fluorescent resorufin (2). We therefore used this reagent to measure H_2O_2 that diffused out of myocardial strips. Inasmuch as plasma interfered with peroxidatic assays, the strips were reconstituted in 2 ml of phenol red-free Hanks' buffered salt solution, added with Amplex Red reagent (80 μM) and horseradish peroxidase (0.11 units/ml). After 4-h incubations in the absence or presence of anthracyclines, the medium was mixed with 1 mM sodium azide to inhibit horseradish peroxidase and was extracted with a 2-fold excess of (1:1) $CHCl_3/CH_3OH$. The methanolic phase of the extracts was analyzed by HPLC to avoid an overlapping of the fluorescence of anthracyclines with that of resorufin (excitation at 485 nm/emission at 595 nm). The HPLC procedure was the same as that described for the DCF assay, except that the mobile phase was adjusted to pH 6.0. Resorufin eluted at 9.8 min, whereas DOX or EPI eluted at 13 min. The assay was calibrated by reacting nanomolar amounts of H_2O_2 with Amplex Red (80 μM), horseradish peroxidase (0.11 units/ml), and by comparing the fluorescence of Amplex Red-derived resorufin with a standard curve of authentic resorufin; one molecule of H_2O_2 was used to generate one molecule of resorufin, and the assay had a detection limit of 2 nM resorufin.

Anthracycline Metabolism Assays in Cell-free Systems—The whole membrane fraction of control myocardial strips (1 mg of protein/ml) was reconstituted with 0.5 mM NADH and 0.1–100 μM anthracyclines,

in the absence or presence of 5 μM DCFH. After 4 h of incubation at 37 °C, the incubations were extracted and assayed for 7-deoxydoxorubicinone, 7-deoxydoxorubicinolone, and DCF. The latter was corrected for DCF formation in incubations that contained only membranes and was quantified against a standard curve of authentic DCF. The soluble fraction of the same strips (0.6 mg protein/ml) was assayed for DOXOL and EPIOL after 4 h of reconstitution with 0.25 mM NADPH and 10–500 μM anthracyclines. Because high levels of DOXOL or EPIOL eventually oxidize with the [4Fe-4S] cluster of cytoplasmic aconitase, all soluble fractions were subjected to cluster disassembly with dithiothreitol, pH 8.9, prior to reconstitution with anthracyclines and NADPH (13). This procedure favored metabolite accumulation and calculations of pertinent kinetics.

Aconitase Assay—Soluble and membrane fractions were isolated in ice-cold 0.3 M NaCl that contained 0.1 mM *cis*-aconitate to minimize an artifactual oxidation of the [4Fe-4S] cluster of aconitases. Next, 30–60 μg of protein/ml were assayed for aconitase activity by monitoring spectrophotometrically the consumption of freshly added 0.1 mM *cis*-aconitate ($\epsilon_{240} = 3.6 \text{ mM}^{-1} \text{ cm}^{-1}$) (13). One unit of aconitase activity was defined as the amount catalyzing the consumption of 1 μmol of *cis*-aconitate per min. Where indicated, the proteins were preincubated for 5 min with cysteine and ferrous ammonium sulfate (1100 or 50 nmol/mg protein, respectively); this was done to reconstitute the [4Fe-4S] cluster of aconitase and obtain maximal enzyme activity (13, 14).

Cell Cultures and Confocal Laser Scanning Inverted Microscopy—We used the H9c2 cell line derived from embryonic BD1X rat heart (CRL 1446; American Type Culture Collection). Cells were grown at 37 °C

TABLE 1

DOX and EPI distribution in human myocardial strips

DOX and EPI were assayed in human myocardial strips as described under "Experimental Procedures." All values were determined at 4 h (means \pm S.E., $n = 3$).

Anthracycline	Membrane fraction	Soluble fraction
	nmol/g	
1 μM		
DOX	0.9 \pm 0.1	1.2 \pm 0.2
EPI	1.2 \pm 0.03	1 \pm 0.2
10 μM		
DOX	5.4 \pm 0.2 ^a	8.5 \pm 0.2 ^a
EPI	8.8 \pm 0.9 ^{a,b}	6.7 \pm 0.6 ^a

^a $p < 0.001$ for 10 μ M DOX or EPI versus 1 μ M in the corresponding fraction.

^b $p < 0.05$ for 10 μ M EPI versus 10 μ M DOX in the membrane fraction.

under 5% CO₂/air in Dulbecco's modified Eagle's medium adjusted to contain 4 mM glutamine, 18 mM sodium bicarbonate, 25 mM glucose, 1 mM sodium pyruvate, 100 units/ml penicillin, and 0.1 ng/ml streptomycin, and supplemented with 10% heat-inactivated fetal calf serum. Subconfluent H9c2 cells (50×10^3) were plated on 25-mm glass coverslips and maintained for 24 h in culture medium. At the time of experiments the medium was removed, and cells were washed twice with Normal External Solution (NES) containing (in mM): 125 NaCl, 5 KCl, 1 MgSO₄, 1 KH₂PO₄, 5.5 glucose, 1 CaCl₂, 20 HEPES, pH 7.4. Next, the cells were incubated for 40 min with 10 μ M DCFH-DA and 100 nM Mito Tracker Deep Red 633, a mitochondrion-specific probe (25). At the end of loading, the cells were washed with NES, transferred into an 1-ml Attofluor[®] (Molecular Probes, Eugene, OR), and examined by a Zeiss LSM510 META confocal system (Jena, Germany) connected to an inverted Zeiss Axiovert 200 microscope equipped with a Plan Neofluar oil-immersion objective ($\times 40/1.3$ NA). After 90 s of equilibration and acquisition of base-line images, 10 or 50 μ M DOX or EPI was added, and the fluorescences of anthracyclines, Mito Tracker Deep Red 633, and DCF were simultaneously monitored every 10 s using an argon laser beam with excitation lines at 488 nm and a helium-neon 633 nm source. To separate emissions of the three fluorochromes, HTF 488/543/633, NTF 545, and NTF 635 primary and secondary dichroic mirrors were used. Detector bandpass filters were set over 505–530 and 565–615 or 663–695 nm ranges for the emissions of DCF (green), anthracyclines (red) and Mito Tracker Deep Red (far red). The latter was pseudocolored dark blue. Attenuation of laser beam intensity and fluorochrome oxidative degradation was obtained through an acoustically and optically regulated filter set on the excitation beam and adjusted to 1% of potency. Where indicated, H9c2 cells were examined after sequential exposure to anthracyclines (50 μ M, 20 min at 37 °C) and the green fluorescent acidotropic probe Lyso Tracker Green DND-26 (100 nM, 40 min at 37 °C). Examination settings were as follows: laser beam at 488 nm with 2% potency, HTF 488/543/633 or NTF 545 primary or secondary dichroic mirrors, bandpass filters at 505–530 or 585–615 nm for the green and red emissions of Lyso Tracker Green DND-26 or anthracyclines, respectively.

Post-acquisition image analyses were carried out with a Zeiss LSM 5 Image Examiner software. Regions of interest were identified of ~ 11 μ m diameter in distinct cells, and their average fluorescence intensities were expressed as $F-F_0/F_0$ ratios, where F_0 and F indicate fluorescences before and after anthracycline addition, respectively. Colocalizations were determined by Image J-Image Correlator Plus Plug-in[®] (NIH Image, Bethesda, MD) and were quantified by Pearson's correlation coefficient; values of 0 indicated no colocalization, and values of 1 indicated complete colocalization (26). All experiments were performed at room temperature, and each coverslip was used for no longer than 30 min.

Other Assays and Conditions—Proteins were measured by the bicinchoninic acid method. Myocardial release of myoglobin, troponin T, and creatine kinase isoenzyme MB was determined by electrochemiluminescence immunoassay with an Elecsys 2010 Analyzer (Roche Diagnostics), according to manufacturer's instructions. Unless otherwise indicated all values were means \pm S.E. of three experiments. Data were analyzed by one-way analysis of variance followed by Bonferroni's test for multiple comparisons; differences were considered significant when p was < 0.05 . Other details are given under "Results" or in the figure legends.

RESULTS

Characterization of a Translational Model of Human Heart—Human myocardial strips were exposed to 1 and 10 μ M anthracyclines. These concentrations were severalfold lower than in previous studies of rabbit isolated heart (10, 11) but ranged over levels measured in the plasma of patients shortly after standard boluses of DOX (27) or EPI (28). Moreover, all experiments were reconstituted in fresh plasma from healthy donors to account for the known ability of albumin and α -acid glycoprotein to bind anthracyclines and limit their partitioning in tissues (29). Under such defined conditions 1–10 μ M DOX or EPI never caused myocardial damage and release of myoglobin, troponin T, and creatine kinase isoenzyme MB, which only occurred when anthracyclines were used at suprapharmacological concentrations like 100 μ M (not shown).

Anthracycline Steady-state Levels and Distribution in Human Myocardium—Human myocardial strips exhibited comparable concentration dependent steady-state levels of DOX and EPI (nmol/g wet weight/4 h, 1.8 \pm 0.3 versus 2.1 \pm 0.1 and 13.9 \pm 0.3 versus 16 \pm 0.9 at 1 and 10 μ M, respectively; $n = 3$). Because human myocardium has the same density of water (10, 11), the concentrations of DOX or EPI in the strips formally exceeded those added in plasma by factors ranging from 1.4 to 2.1. These results were consistent with the known ability of cardiac tissue to accumulate anthracyclines; however, the accumulation factors determined in this study were significantly lower than those determined by others when studying isolated heart preparations in common laboratory buffers (factors ≥ 3 ; see Ref. 10). This denoted the ability of plasma proteins to limit the diffusion of anthracyclines in myocardial strips. The distribution of DOX and EPI in the soluble and membrane fractions of the strips followed a similar concentration-dependent pattern, but 10 μ M EPI showed a higher level of distribution in the membrane fraction as compared with equimolar DOX (Table 1).

Epirubicin Does Not Form H₂O₂ in Human Myocardium—In previous studies anthracycline-dependent ROS formation was determined by means of the DCF assay (15, 30–33). This method is said to monitor oxidation of DCFH by H₂O₂ and cellular peroxidases or pathophysiological traces of iron (21, 30), but alternative mechanisms of oxidation or potential pitfalls have been described (21, 34). Moreover, a quantitative relation between the redox cycling of anthracyclines and the levels of DCF formation was not established. We considered these concerns and performed preliminary experiments that characterized the H₂O₂ dependence of the DCF assay. In the first set of experiments human myocardial strips were assayed for DCF after 4 h of incubation in plasma, in the absence or presence of 100 μ M antimycin A or 50 mM aminotriazole. Antimycin A was used to inhibit complex III in the respiratory chain and induce a leakage of H₂O₂ from mitochondria, whereas aminotriazole was used to inhibit catalase and reduce H₂O₂ decomposition (23). Both antimycin A and aminotriazole increased DCF formation in the strips (4.3 or 2.6 times, respectively), and this was caused by concomitant increases of DCF in the soluble or membrane

Epirubicin and Mechanisms of Anthracycline Cardiotoxicity

TABLE 2

Intracellular, extracellular, and total H₂O₂ levels in control or anthracycline-treated human myocardial strips

Values were means ± S.E. of six experiments.

Myocardial sample	Intracellular H ₂ O ₂ ^a		Extracellular H ₂ O ₂ ^b	Total H ₂ O ₂ ^c
	Membrane fraction	Soluble fraction		
Control	0.3 ± 0.01	0.05 ± 0.02	0.021 ± 0.002	0.38 ± 0.01
+ 1 μM anthracycline				
DOX	0.8 ± 0.2*	0.03 ± 0.01	0.051 ± 0.005†	0.90 ± 0.2††
EPI	0.3 ± 0.1	0.04 ± 0.01	0.023 ± 0.005	0.34 ± 0.1
+ 10 μM anthracycline				
DOX	1 ± 0.1**	0.04 ± 0.01	ND ^d	ND
EPI	0.3 ± 0.1	0.03 ± 0.01	ND	ND

^a Myocardial strips were loaded with DCFH-DA and reconstituted in plasma in the absence or presence of 1 or 10 μM DOX or EPI. Membrane and soluble fractions were assayed for DCF-detectable H₂O₂, which was quantified based upon a stoichiometry of 0.43 ± 0.07 nmol of DCF per nmol of H₂O₂ (see "Experimental Procedures"). *p* < 0.05 (*) and *p* < 0.01 (**) versus control (*p* > 0.05 for 1 versus 10 μM DOX).

^b Myocardial strips were reconstituted in phenol red-free Hanks' buffered salt solution added with Amplex Red reagent (80 μM) and horseradish peroxidase (0.11 units/ml), in the absence or presence of 1 μM DOX or EPI. Extracellular H₂O₂ was measured as resorufin formation, as described under "Experimental Procedures." Values (nmol/ml) were eventually normalized to gram of myocardial tissue. †, *p* < 0.01 versus control.

^c Data are calculated as the sum of individual values of intracellular H₂O₂ (membrane fraction + soluble fraction) and extracellular H₂O₂. ††, *p* < 0.01 versus control.

^d ND indicates not determined because of interferences of 10 μM anthracyclines with the fluorescence of resorufin in the Amplex Red reagent assay for extracellular H₂O₂.

fractions. Moreover, combining antimycin A and aminotriazole further increased DCF formation as compared with either agent alone (not shown).

These results showed that the DCF assay sensed H₂O₂ that diffused across soluble and membrane fractions of myocardial strips. Therefore, we titrated the strips with 0.1–10 μM H₂O₂ and determined that 1 nmol of exogenous H₂O₂ caused the net formation of 0.43 nmol of DCF/g of myocardial tissue (see under "Experimental Procedures"). The lack of a 1:1 stoichiometry of H₂O₂ versus DCF could be attributed to incomplete diffusion or retention of H₂O₂ in the strips or, more likely, to H₂O₂-independent oxidation of DCFH or side reactions of DCF with redox-active cell constituents (21, 34).

Having characterized the H₂O₂ dependence and stoichiometry of the DCF assay, we quantified basal or anthracycline-induced H₂O₂ formation in myocardial strips exposed to 1 or 10 μM anthracyclines. Under basal conditions, the levels of H₂O₂ in the membrane fraction were ~6-fold those in the soluble fraction (0.3 ± 0.01 versus 0.05 ± 0.02 nmol/g/4 h) (Table 2, 1st column). Doxorubicin, but not EPI, significantly increased H₂O₂ in the membrane fraction. The effect of DOX showed a trend toward a concentration dependence, but the difference between 1 and 10 μM DOX did not prove statistically significant within the sample size of this study. Neither DOX nor EPI increased H₂O₂ in the soluble fraction; if anything, both anthracyclines caused a slight although not significant decrease of H₂O₂ (see also Table 2, 1st column). Soluble and membrane fractions of anthracycline-treated strips were assayed for DCF also after incubation with a strong excess of H₂O₂ (1 mM), a procedure aimed at oxidizing any residual DCFH. All samples showed remarkable increases of DCF (from a minimum of 270% in membrane fractions up to a maximum of 600% in soluble fractions) (data not shown). This demonstrated that neither the lack of H₂O₂ formation in the membrane fractions of EPI-treated samples nor the lack of H₂O₂ formation in the soluble fractions of DOX- or EPI-treated samples could be attributed to a limited availability of DCFH in those particular samples. Oxidation of the Amplex Red reagent to fluorescent resorufin was used as a biochemical index of H₂O₂ that diffused out of myocardial strips during the course of the experiments (24). Under basal conditions the strips released 0.021 ± 0.002 nmol H₂O₂/g/4 h, *i.e.* ~40% of H₂O₂ that was recovered in the soluble fraction. One micromolar DOX more than doubled H₂O₂ that diffused out of the strips, whereas equimolar EPI caused no change (Table 2, 2nd column). The effects of 10 μM DOX or EPI could not be determined because >1 μM anthracyclines quenched the fluorescence of resorufin (not shown).

By having assayed myocardial strips for both intra- and extracellular H₂O₂, we quantified the total levels of H₂O₂ and compared them to a physiologic range of H₂O₂ concentrations that, in many cell types, was approximated to 0.1–0.01 μM (35). Under basal conditions, total H₂O₂ averaged 0.38 ± 0.01 nmol/g/4 h (0.38 μM if one considered that human myocardium has the same density of water) (Table 2, 3rd column). In the light of factors such as the low antioxidant defenses of the heart, and the different procedures adopted to measure intra- or extracellular H₂O₂ in separate studies (35), 0.38 μM H₂O₂ compared reasonably well with the upper limit of the physiologic range of H₂O₂ concentrations. One micromolar EPI did not modify H₂O₂ levels, whereas equimolar DOX raised them to 0.90 ± 0.2 nmol/g/4 h (or micromolar equivalents) (see also Table 2, 3rd column).

These results suggested that human myocardium reduced DOX, but not EPI, to a semiquinone able to oxidize with oxygen and form H₂O₂ or other ROS. As mentioned, anthracycline semiquinones can also disproportionate and rearrange to 7-deoxydoxorubicinolone through a concomitant deglycosidation and reduction of the side chain carbonyl group (*cf.* Fig. 1). We therefore measured 7-deoxydoxorubicinolone as an additional marker of the redox cycling of anthracyclines in soluble or membrane fractions of myocardial strips. As shown in Fig. 2 7-deoxydoxorubicinolone was found in the membrane fraction of myocardial strips exposed to 1 μM DOX but not in those exposed to equimolar EPI. The soluble fractions contained trace amounts of 7-deoxydoxorubicinolone, but this was seen with both DOX and EPI and could not be attributed to a typical redox cycling. In fact, experiments with cell-free systems showed that the soluble fraction contained reductases that sequentially deglycosylated anthracyclines to 7-deoxydoxorubicinone and reduced the latter to 7-deoxydoxorubicinolone, without any redox cycling of the quinone (not shown). Accordingly, the soluble fractions always contained residues of 7-deoxydoxorubicinone, whereas the membrane fractions did not contain measurable 7-deoxydoxorubicinone (see also Fig. 2).

By combining the assays for DCF and 7-deoxydoxorubicinolone, we concluded that DOX redox cycled and formed H₂O₂ in the membrane fraction of myocardial strips. Hydrogen peroxide likely diffused from membranes in the soluble fraction, but the latter never exhibited a measurable increase of H₂O₂. This finding was at least in part attributable to an extracellular diffusion of H₂O₂ (see Table 2); it is also possible that some H₂O₂ was eliminated through the pseudoperoxidatic activity of myoglobin, which is highly abundant in cytosol and utilizes anthra-

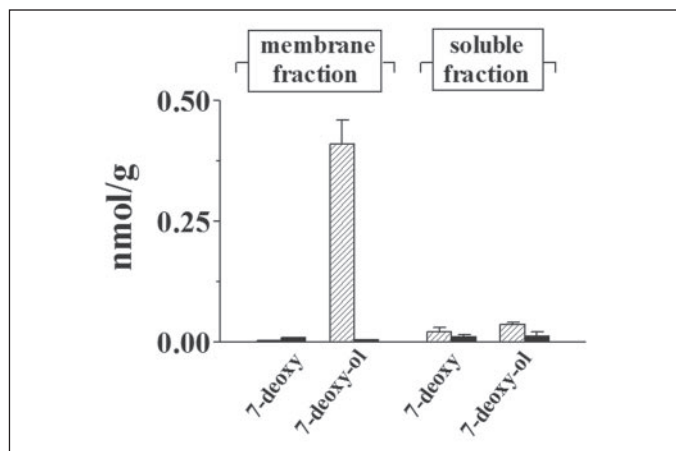


FIGURE 2. Formation of 7-deoxydoxorubicinolone in human myocardial strips exposed to DOX or EPI. Myocardial strips were reconstituted in plasma with $1 \mu\text{M}$ DOX or EPI and assayed for 7-deoxydoxorubicinolone or 7-deoxydoxorubicinolone, as described under "Experimental Procedures." Values were means \pm S.E. of three experiments. 7-Deoxy, 7-deoxydoxorubicinolone; 7-deoxy-ol, 7-deoxydoxorubicinolone.

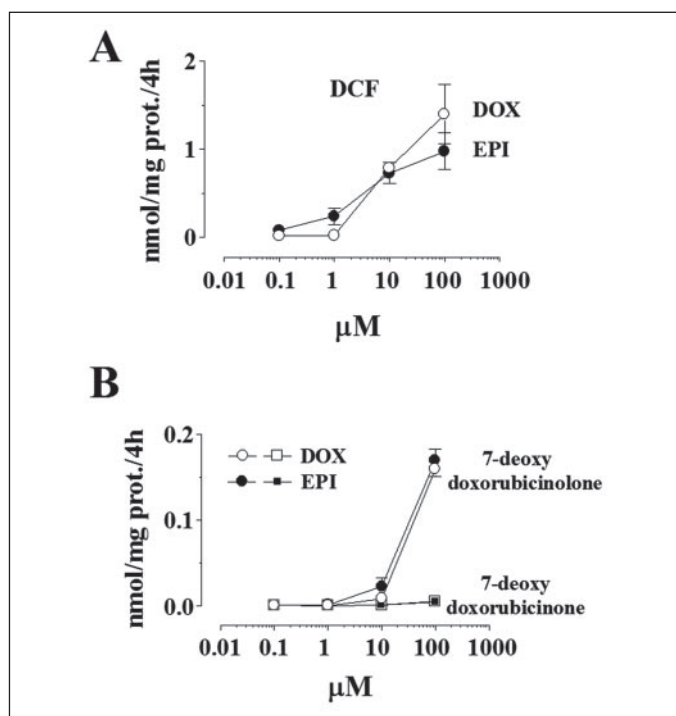


FIGURE 3. Redox cycling of DOX or EPI in cell-free systems. The incubations (0.2 ml) contained the whole membrane fractions of control human myocardial strips (1 mg/ml), 0.1–100 μM DOX or EPI, 5 μM DCFH, and NADH (0.5 mM). A shows oxidation of DCFH to DCF; values were corrected for the levels of DCF in incubations containing only membranes and were quantified against a standard curve of authentic DCF. B shows the formation of 7-deoxydoxorubicinolone or 7-deoxydoxorubicinolone. Values were means \pm S.E. of three experiments.

cyclines as reducing substrates (36). Epirubicin did not undergo redox cycling and consequently failed to increase intra- or extracellular levels of H_2O_2 .

Redox Cycling of Epirubicin in Cell-free Systems—Doxorubicin and EPI were probed in cell-free systems that contained the membrane fraction of control strips and NADH as a cofactor. In these systems both DOX and EPI caused the oxidation of DCFH to DCF (Fig. 3A), or converted to 7-deoxydoxorubicinolone without formation of 7-deoxydoxorubicinolone (Fig. 3B).

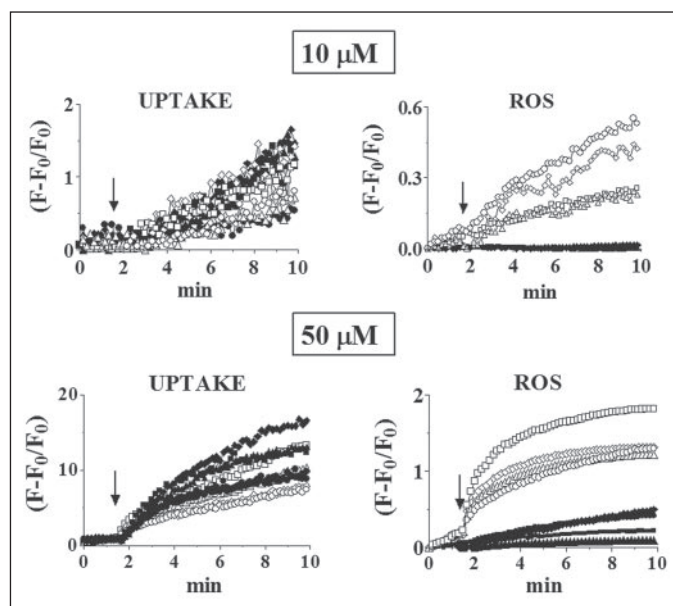


FIGURE 4. Anthracycline uptake and ROS formation in H9c2 cardiomyocytes. Four different preparations of H9c2 cardiomyocytes were analyzed by confocal laser scanning microscopy following loading with DCFH-DA and exposure to 10 or 50 μM DOX (\square , \diamond , \triangle) or EPI (\bullet , \blacklozenge , \blacktriangle). Anthracycline addition is indicated by arrows. Drug uptake and DCF-detectable ROS formation were monitored simultaneously and expressed as $F - F_0/F_0$, where F_0 and F indicate fluorescences before and after anthracycline addition, respectively (see "Experimental Procedures").

Vesicular Sequestration Limits Epirubicin-dependent ROS Formation in H9c2 Cardiomyocytes—Mitochondrial NADH dehydrogenases, such as the NADH:ubiquinone oxidoreductase (37) and the so-called "exogenous" NADH dehydrogenase (8), rank among the most effective catalysts of anthracycline redox cycling in the heart. The failure of EPI to redox cycle in human myocardial strips, as opposed to its efficient redox cycling in NADH-supplemented cell-free systems, suggested that EPI might exhibit an altered cellular trafficking that limited its access to mitochondria. One such possibility had to be reconciled with the fact that the levels of EPI in the whole membrane fraction of the strips were equal to or higher than those of DOX (see Table 1). We considered that EPI could have been distributed in membrane compartments other than mitochondria and that such redistribution required measuring EPI in individual cellular organelles rather than in a whole membrane fraction. Limitations in the number and size of myocardial samples did not allow us to adopt this procedure without avoiding potential pitfalls like artifactual cosedimentation of anthracyclines with partly damaged organelles, for example.

To obtain pertinent information while obviating the aforesaid limitations, we used confocal microscopy and monitored anthracycline uptake and distribution or ROS formation in H9c2 cardiomyocytes, a cell line that proved highly convenient in previous studies of anthracycline-dependent ROS formation (15, 31–33). These experiments were conducted with 10 and 50 μM DOX or EPI to optimize visualization of anthracyclines and to characterize the concentration dependence of their effects; however, these concentration levels did not affect cell viability within the experiment time (not shown). As reported in Fig. 4, DOX (*open symbols*) exhibited a concentration- and time-dependent uptake in H9c2 cardiomyocytes, which was accompanied by a similar pattern of DCF-detectable ROS formation. Under comparable conditions EPI (*solid symbols*) exhibited a similar uptake but formed no ROS at 10 μM or much less ROS than DOX at 50 μM .

We next loaded cardiomyocytes with both DCFH-DA and the mitochondrion-specific probe Mito Tracker Deep Red 633. The latter was

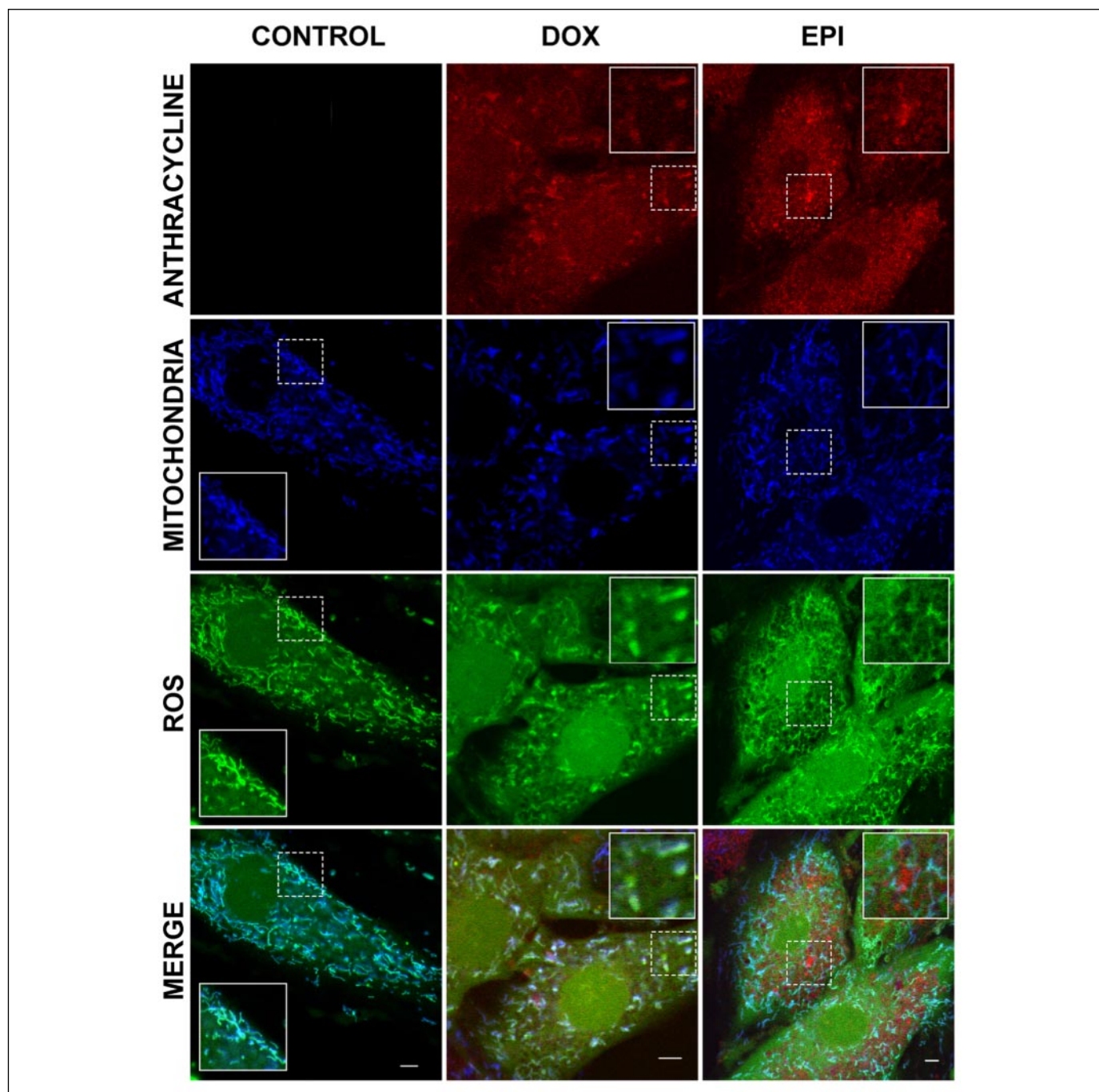


FIGURE 5. **Anthracycline-mitochondria colocalizations and ROS formation in H9c2 cardiomyocytes.** H9c2 cardiomyocytes were analyzed by confocal microscopy after loading with DCFH-DA and the mitochondrial stain Mito Tracker Deep Red 633, pseudocolored dark blue ("Experimental Procedures"). Where indicated cardiomyocytes were exposed to 50 μM DOX or EPI. Areas of interest were identified (dashed squares) and magnified (solid squares). Images were recorded 10 min after base-line equilibration and anthracycline addition. This set of data is representative of four experiments. Scale bar, 20 μm .

chosen because its fluorescence is only marginally sensitive to modifications of the mitochondrial redox status (38); therefore, Mito Tracker Deep Red 633 offered a stable mitochondrial staining if these organelles formed basal or anthracycline-induced levels of ROS during the course of the experiment.

In control cells mitochondria were stained by Mito Tracker Deep Red 633 in a web-like conformation; moreover, there was a good overlapping of the dark blue pseudocolor of Mito Tracker Deep Red with the green fluorescence of DCF, indicating that mitochondria formed a basal level of H_2O_2 or other ROS (Fig. 5, left panels and insets with magnifications of areas of interest). In experiments with 50 μM DOX, many anthracy-

cline-ROS-mitochondria colocalizations were observed, which resulted in a good merging of the red fluorescence of the anthracycline with the dark blue pseudocolor of Mito Tracker Deep Red 633 and the green fluorescence of DCF. These colocalizations were accompanied by modifications of mitochondria, which lost their web-like shape but exhibited a "sausage"-like shape (Fig. 5, central panels and insets). Equimolar EPI did not show this pattern but formed vesicle-like spots that did not colocalize with mitochondria or ROS; moreover, the mitochondria of cardiomyocytes exposed to EPI were shaped more similar to those of control cells (Fig. 5, right panels and insets). Comparable results were obtained with 10 μM anthracyclines (not shown).

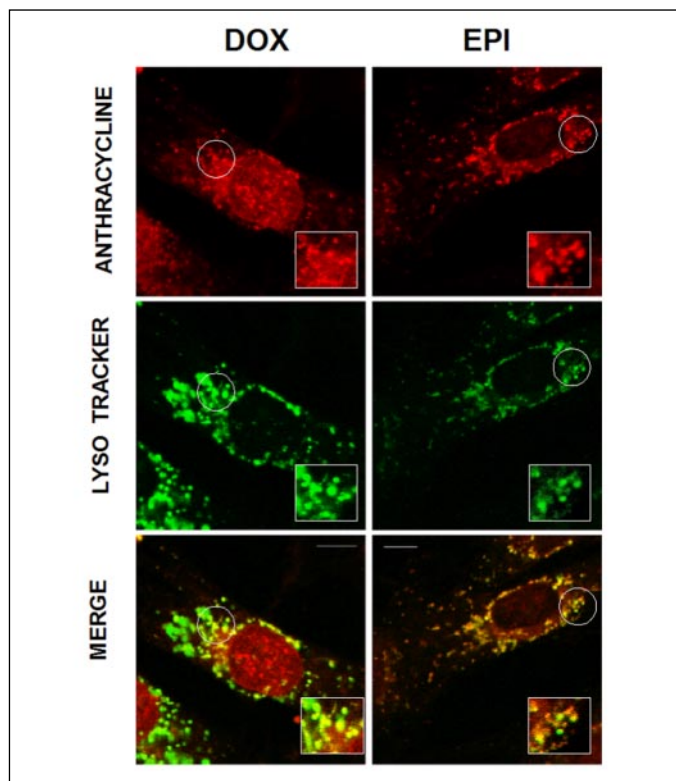


FIGURE 6. Anthracycline accumulation in cytoplasmic acidic organelles of H9c2 cardiomyocytes. H9c2 cardiomyocytes were visualized by confocal microscopy after sequential loading with anthracyclines ($50 \mu\text{M}$) and the acidotropic probe Lyso Tracker Green DND-26. Areas of interest were circled and magnified in square insets. This set of data is representative of three experiments. Scale bar, $50 \mu\text{m}$.

Anthracyclines are known to diffuse into cytoplasmic acidic organelles (lysosomes, recycling endosomes, and vesicles of the *trans*-Golgi network). The low pH of these organelles causes protonation of the basic amino residue of daunosamine, rendering anthracyclines less membrane-permeable and favoring their accumulation in the vesicles (39–41). We therefore determined whether the vesicle-like spots of EPI were indicative of its protonation-sequestration in cytoplasmic acidic organelles. To obtain this information we used Lyso Tracker Green DND-26, a membrane-permeable probe that is only partially protonated at neutral pH and gains green fluorescence upon further protonation and retention in the acidic vesicular apparatus (42). In preliminary experiments (not shown), we found that H9c2 cardiomyocytes loaded with this probe exhibited a widely distributed green punctate fluorescence that gradually disappeared upon addition of bafilomycin A1, a specific inhibitor of the vacuolar H^+ -ATPase that acidifies cytoplasmic organelles (43). We next loaded cardiomyocytes with both Lyso Tracker Green DND-26 and $50 \mu\text{M}$ anthracyclines. Merged images of DOX-treated cardiomyocytes showed only few yellow spots that indicated a modest colocalization of the anthracycline with Lyso Tracker Green DND-26; in contrast, EPI-treated cardiomyocytes exhibited numerous and widely distributed yellow-brownish spots that indicated a much stronger colocalization of the anthracycline with the acidotropic probe (Fig. 6, insets). These results demonstrated that EPI was remarkably more susceptible than DOX to protonation-sequestration in cytoplasmic acidic organelles.

We characterized whether the failure of EPI to reach mitochondria and form ROS in H9c2 cardiomyocytes was caused by its sequestration in cytoplasmic acid organelles. To obtain this information we exposed cardiomyocytes to bafilomycin overnight and during subsequent expo-

sure to $50 \mu\text{M}$ EPI, in order to inhibit organellar acidification and abolish the protonation-sequestration mechanism. 20 nM bafilomycin was used, a concentration level that did not affect cell viability within the experiment time (not shown). Under such defined conditions, bafilomycin caused the appearance of large vacuoles that are typical of cytoplasmic organelles subjected to a disruption of their transmembrane pH gradient (44). These changes were accompanied by the presence of minor residues of EPI in the vacuoles, mostly in the form of apical aggregates, and by the appearance of numerous EPI-mitochondria-ROS colocalizations (Fig. 7, inset A). Bafilomycin had essentially no effect on the usual pattern of DOX-mitochondria-ROS colocalizations (not shown); moreover, the vacuoles of cells sequentially exposed to bafilomycin and DOX did not contain anthracycline residues (cf. Fig. 7, inset B).

On the basis of these findings, we calculated the efficiency with which DOX or EPI formed ROS in control or bafilomycin-treated cardiomyocytes. This was done by normalizing ROS formation to anthracycline uptake in cardiomyocytes, thus obviating unavoidable differences in intracellular drug levels among multiple sets of experiments with control or bafilomycin-treated cells. Doxorubicin exhibited an efficiency of ROS formation that only marginally increased in response to pretreatment with bafilomycin; EPI exhibited a much lower efficiency, but this increased severalfold after bafilomycin treatment and became similar to that of DOX (Fig. 8A). The same pattern occurred with anthracycline-mitochondria colocalizations, expressed by the Pearson's coefficient. In the absence of bafilomycin the coefficient of DOX-mitochondria colocalizations was three times higher than that of EPI-mitochondria colocalizations (0.52 versus 0.18); this was in keeping with the fact that DOX-mitochondria-ROS colocalizations were accompanied by shape changes of the organelles, whereas in EPI-treated cells the mitochondrial shape was more similar to that seen in control cells (cf. Fig. 5). Bafilomycin only marginally increased DOX-mitochondria colocalizations but increased EPI-mitochondria colocalizations by 4.5-fold (Fig. 8B); the latter finding was in agreement with the fact that the mitochondria of cells treated with EPI + bafilomycin lost their web-like shape and became more similar to the sausage-like mitochondria of DOX-treated cells (see Fig. 7). Finally, the efficiencies of ROS formation correlated in a highly significant manner with anthracycline-mitochondria colocalizations in control or bafilomycin-treated cells (Fig. 8C).

Collectively, the experiments in Figs. 4–8 showed the following: (i) DOX and EPI exhibited the same uptake in H9c2 cardiomyocytes; (ii) only DOX localized to mitochondrial sites of redox cycling and ROS formation; (iii) EPI could not form ROS because of its sequestration in cytoplasmic acidic organelles and limited access to mitochondria; and (iv) inhibition of the vacuolar H^+ -ATPase prevented the vesicular sequestration of EPI and increased its localization to mitochondria.⁵

Inhibition of Vacuolar H^+ -ATPase Increases Epirubicin-dependent H_2O_2 Formation in Human Myocardium—We characterized whether the protonation-sequestration mechanism also occurred in human myocardium and caused the failure of EPI to redox cycle at mitochondrial sites. For this purpose myocardial strips were exposed to bafilomycin during loading with DCFH-DA and subsequent exposure to $10 \mu\text{M}$ anthracyclines. Under such defined conditions bafilomycin had no effect on the net increase of DCF-detectable H_2O_2 equivalents induced by DOX; this was in keeping with the fact that only few molecules of

⁵ Note that EPI exhibited also a reduced nuclear partitioning as compared with DOX (cf. Figs. 5 and 6). Bafilomycin treatment and consequent inhibition of vesicular sequestration improved the partitioning of EPI in the nucleus (Fig. 7).

FIGURE 7. Effects of bafilomycin on EPI distribution and ROS formation in H9c2 cardiomyocytes. Bafilomycin-treated H9c2 cardiomyocytes were visualized by confocal microscopy after loading with DCFH-DA and Mito Tracker Deep Red and subsequent exposure to 50 μM EPI. The arrows indicate colocalizations of EPI with mitochondria and mitochondria-associated ROS formation. The insets show minute anthracycline residues in the vacuoles of cardiomyocytes treated with EPI (A) but not in those treated with DOX (B). Images were recorded 10 min after anthracycline addition. This set of data is representative of three experiments. Scale bar, 50 μm .

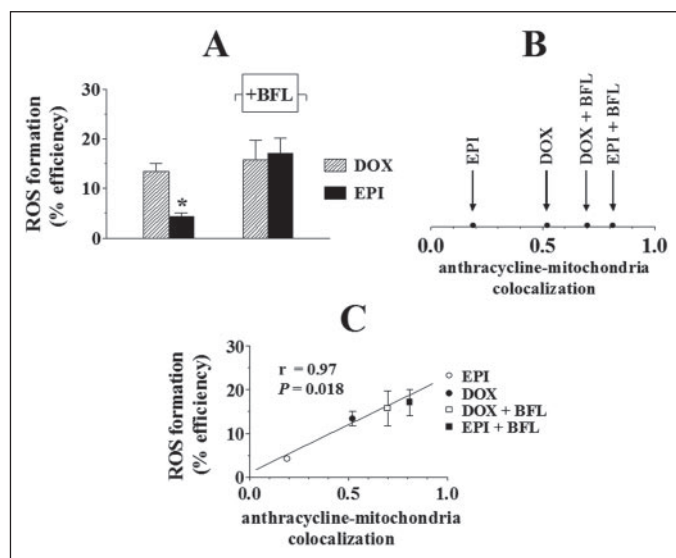
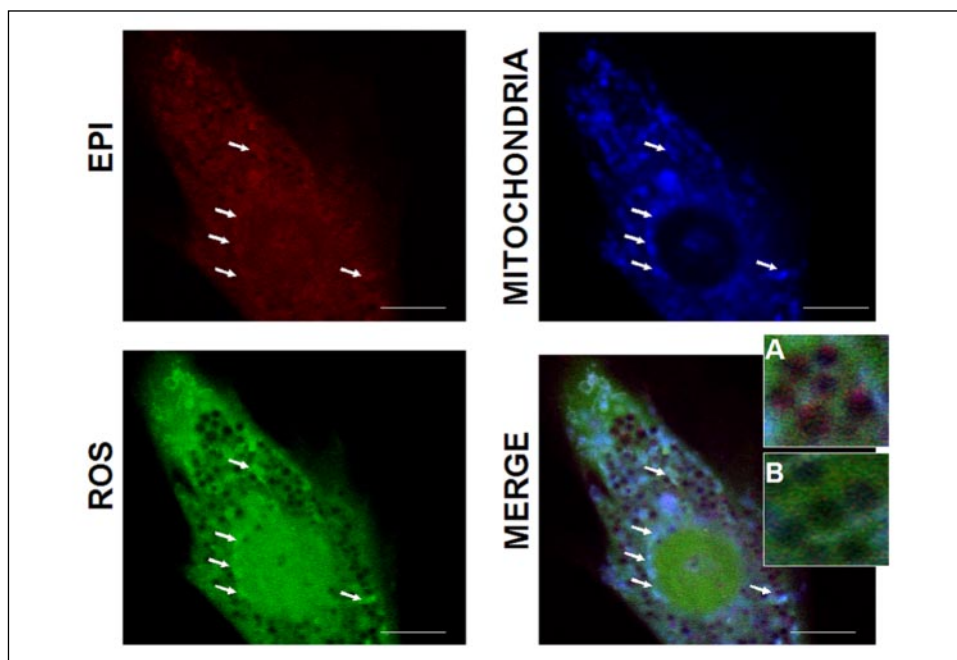


FIGURE 8. Anthracycline-mitochondria colocalizations and efficiency of ROS formation in H9c2 cardiomyocytes. A shows the efficiency of DCF-detectable ROS formation induced by 50 μM DOX or EPI in control or bafilomycin-treated H9c2 cardiomyocytes. Values were means \pm S.E. of 5–10 regions of interest and were determined by normalizing $(F - F_0/F_0)$ ratios of DCF to $(F - F_0/F_0)$ ratios of anthracyclines (the asterisk indicates $p < 0.05$ for EPI versus all other samples). B shows anthracycline-mitochondria colocalizations (Pearson's coefficient) in the same cells, and C shows the correlation of colocalizations with the efficiencies of ROS formation. BFL, bafilomycin.

DOX underwent protonation-sequestration. In contrast, bafilomycin increased H_2O_2 formation by EPI, which reached the same level as that of DOX. All such effects were confined to the membrane fraction of myocardial strips; bafilomycin had no effect in the soluble fraction, in which both DOX and EPI were confirmed to cause a slight decrease of H_2O_2 formation (Fig. 9A). Of note, bafilomycin did not modify the steady-state levels of DOX in the strips (nmol/g/4 h: 14.1 ± 1.8 versus a control value of 13.9 ± 0.3), but decreased those of EPI from 16.1 ± 0.9 to 9.6 ± 0.8 nmol/g/4 h ($n = 3$, $p < 0.01$). The latter effect was caused by a significant decrease of EPI in the soluble fraction (from 6.7 ± 0.6 to 2.9 ± 0.4 nmol/g/4 h; $n = 3$; $p < 0.01$) and by a more modest decrease in

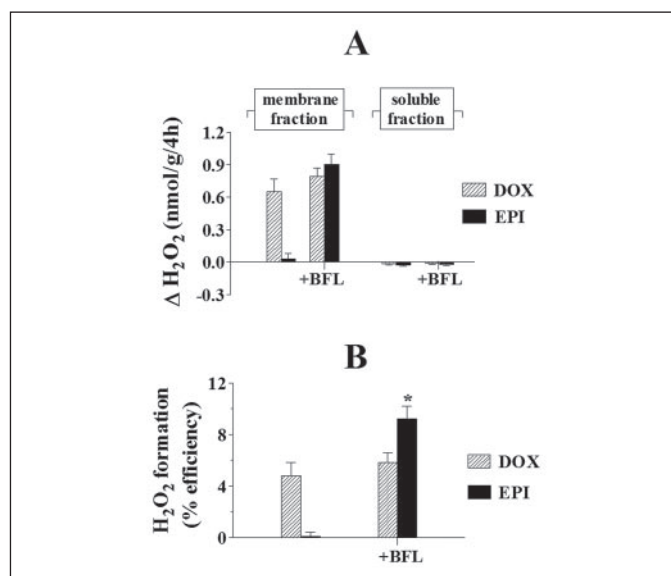


FIGURE 9. Effects of bafilomycin on anthracycline-dependent H_2O_2 formation in human myocardial strips. A, human myocardial strips were loaded with DCFH-DA, reconstituted in plasma with 10 μM anthracyclines, and assayed for DCF-detectable H_2O_2 equivalents in membrane or soluble fractions. Where indicated the strips were also exposed to bafilomycin (300 or 90 nM during loading with DCFH-DA or subsequent incubation in plasma, respectively). Bafilomycin was used dissolved in dimethyl sulfoxide. Values (means \pm S.E. of three experiments) were expressed as net increases (Δ) of H_2O_2 relative to control strips exposed to dimethyl sulfoxide or bafilomycin-dimethyl sulfoxide. B shows the efficiency of H_2O_2 formation induced by DOX or EPI in the absence or presence of bafilomycin; values were obtained by normalizing H_2O_2 increase to anthracycline uptake (nmol/nmol/g of tissue). The asterisk indicates $p < 0.05$ for EPI + bafilomycin versus all other samples. BFL, bafilomycin.

the membrane fraction (from 8.8 ± 0.9 to 6.6 ± 0.5 nmol/g/4h; $n = 3$; $p > 0.05$). The observation that bafilomycin could increase the conversion of EPI to H_2O_2 in the face of its reduced uptake and/or retention in the cardiac tissue implied that EPI had redistributed from sequestration sites toward membrane compartments where it redox cycled in a highly efficient manner. Normalizing the net increases of H_2O_2 formation to the uptake of DOX or EPI therefore showed that EPI *per se* exhibited the lowest efficiency of H_2O_2 formation, but this increased to the highest

TABLE 3

Aconitase activity in membrane and soluble fractions of control- or anthracycline-treated human myocardial strips

Myocardial strips were incubated in plasma, in the absence or presence of 10 μM DOX or EPI. Where indicated the strips were also treated with dimethyl sulfoxide-dissolved bafilomycin (300 nM during 1 h of incubation in 50 mM phosphate buffer, 123 mM NaCl, 5.6 mM glucose, pH 7.4, and 90 nM during subsequent incubation in plasma). After 4 h, membrane and soluble fractions were isolated in 0.3 M NaCl supplemented with 0.1 mM *cis*-aconitate to minimize an artifactual oxidation of the [4Fe-4S] cluster of aconitase. Enzyme activity was assayed as described under "Experimental Procedures"; where indicated aconitase was assayed after reactivation with cysteine and ferrous ammonium sulfate, as also described under "Experimental Procedures." Bafilomycin treatment *per se* had no effect on aconitase activity. Values were means \pm S.E. of three experiments.

Myocardial sample	Membrane fraction		Soluble fraction	
	Basal	Reactivated	Basal	Reactivated
	<i>units of aconitase/g</i>		<i>units of aconitase/g</i>	
Control	0.38 \pm 0.05	0.76 \pm 0.06 ^a	0.05 \pm 0.01	0.08 \pm 0.02
+ 10 μM DOX	0.21 \pm 0.03 ^b	0.72 \pm 0.07 ^a	0.06 \pm 0.01	0.07 \pm 0.01
+ 10 μM DOX + bafilomycin	0.22 \pm 0.04 ^b	0.75 \pm 0.04 ^a	0.06 \pm 0.01	0.07 \pm 0.01
+ 10 μM EPI	0.35 \pm 0.03	0.66 \pm 0.03 ^a	0.05 \pm 0.01	0.07 \pm 0.02
+ 10 μM EPI + bafilomycin	0.19 \pm 0.04 ^b	0.71 \pm 0.05 ^a	0.05 \pm 0.01	0.08 \pm 0.02

^a $p < 0.01$ versus the corresponding basal activity.

^b $p < 0.05$ versus control.

level among all samples examined if the strips had been exposed to bafilomycin (Fig. 9B).

Inactivation of Mitochondrial Aconitase as a Marker of Superoxide Formation by Doxorubicin but Not Epirubicin—Mitochondrial and cytoplasmic aconitases function by virtue of a [4Fe-4S] cluster that is attacked by O_2^- with estimated rates of $\sim 10^7 \text{ M}^{-1} \text{ s}^{-1}$ (45). This is accompanied by release of the solvent-exposed fourth iron atom, oxidation of the cluster, and loss of aconitase activity, but in the absence of any further damage the enzyme can be reactivated with iron and reducing agents (13, 14). Oxygen and H_2O_2 are much less reactive with the cluster ($k = \sim 10^2 \text{ M}^{-1} \text{ s}^{-1}$); hence, aconitase inactivation may serve a rather specific marker of O_2^- formation and reactivity in biologic samples (46). We measured aconitase activities in the membrane and soluble fraction of human myocardial strips that had been incubated in plasma in the absence or presence of anthracyclines. As shown in Table 3 the membrane fraction exhibited much more aconitase activity than the soluble fraction, in keeping with the high mitochondrial density of the heart. Treatment with 10 μM DOX caused a significant loss of aconitase activity in the membrane fraction, regardless of a concomitant administration of bafilomycin. Ten micromolar EPI did not inactivate aconitase, unless the strips had been treated with bafilomycin to prevent its vesicular sequestration. Membrane fractions were assayed for aconitase also after reactivation with cysteine and ferrous ammonium sulfate, a procedure aimed at reassembling the [4Fe-4S] cluster. This treatment increased aconitase activity by ~ 2 – 3.5 -fold in all fractions examined and blunted differences between control or anthracycline-treated samples (see Table 3). Under comparable conditions neither DOX nor EPI or EPI + bafilomycin decreased aconitase activity in the soluble fraction; moreover, treatment with cysteine and ferrous ammonium sulfate caused a less evident increase of aconitase activity, which was not statistically significant within the sample size of this study (see Table 3).

Collectively, these results showed the following: (i) the membrane fraction was the prevailing site of O_2^- formation in myocardial strips; (ii) basal fluxes of O_2^- caused a reversible inactivation of mitochondrial aconitase; (iii) DOX increased O_2^- formation and consequently increased the extent of aconitase reversible inactivation; (iv) EPI could not form O_2^- or inactivate aconitase because of its sequestration in cytoplasmic acidic organelles. This pattern of O_2^- formation was therefore similar to that described for H_2O_2 formation.

Epirubicin Forms Less Alcohol Metabolite than DOX in Human Myocardium—Secondary alcohol metabolites were found only in the soluble fraction of myocardial strips exposed to 10 μM anthracycline, but the levels of EPIOL were $\sim 60\%$ lower than those of DOXOL (Fig. 10). The reduced formation of EPIOL versus DOXOL could not be

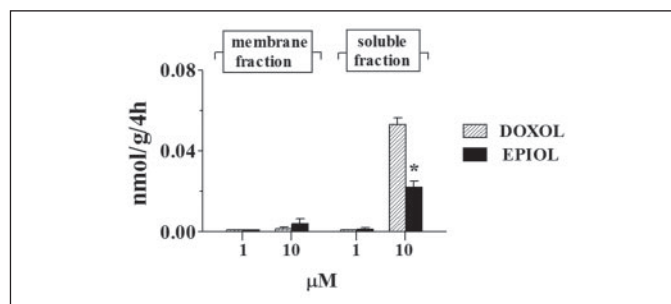


FIGURE 10. Formation of anthracycline secondary alcohol metabolites in human myocardial strips. Doxorubicinol and EPIOL were assayed after 4 h of reconstitution of human myocardial strips in plasma with 1 or 10 μM DOX or EPI (the asterisk indicates $p < 0.001$ for DOXOL versus EPIOL; means \pm S.E., $n = 3$).

attributed to the protonation-sequestration mechanism. In fact, the levels of EPI in the soluble fraction of the strips were similar to those of DOX (see Table 1); moreover, blocking the protonation-sequestration mechanism with bafilomycin did not change the levels of DOXOL formation but decreased those of EPIOL from 0.022 ± 0.003 to 0.009 ± 0.002 (nmol/g/4 h, $p < 0.05$). The latter finding was in keeping with the fact that bafilomycin did not increase but actually decreased the pool of EPI in the soluble fraction of myocardial strips.

H9c2 cardiomyocytes were of limited value in characterizing the different metabolic behavior of EPI versus DOX, as they neither gave the same EPIOL:DOXOL ratios found in the soluble fraction of human myocardial strips nor did they reproduce the pattern of metabolite distribution in soluble versus membrane fraction. In fact, the levels of EPIOL in the soluble fraction of H9c2 cardiomyocytes were $< 5\%$ those of DOXOL; moreover, sizeable amounts of both DOXOL and EPIOL were found in the membrane fraction of these cells (not shown). This confirmed that non-human models cannot help to predict the levels of formation of secondary alcohol metabolites in the human heart (1).

The different metabolic behavior of DOX and EPI was therefore characterized in a cell-free system that contained the soluble fraction of control myocardial strips, and NADPH as a cofactor of aldo/keto or carbonyl reductases that have been shown to catalyze a two-electron reduction of the side chain carbonyl group of anthracyclines (1, 22, 47). Preliminary experiments with 50 μM DOX or EPI showed that the net level of EPIOL formation remained 62% lower than that of DOXOL (0.6 versus 1.6 nmol/mg protein/4 h), similar to what observed with whole myocardial samples. Kinetic studies at 10–500 μM anthracyclines then showed that the conversion of EPI to EPIOL occurred with higher K_m and lower V_{max} values than the conversion of DOX to DOXOL; hence, the catalytic efficiency (V_{max}/K_m) with which the soluble fraction reduced EPI to EPIOL was ~ 1 order of

Epirubicin and Mechanisms of Anthracycline Cardiotoxicity

TABLE 4

Kinetic and inhibitor studies of anthracycline secondary alcohol metabolite formation in the soluble fraction of human myocardial strips

All incubations contained the soluble fraction of control strips (0.6 mg protein/ml) and 0.25 mM NADPH. Values were means of two separate determinations with >95% experimental agreement.

Anthracycline	K_m^a	V_{max}^b	V_{max}/K_m	IC_{50}^c	
				Tolrestat	Quercetin
	μM	$nmol/mg$ <i>protein/min</i>	$ml/(mg$ <i>protein/min)</i>	μM	
DOX	79	0.014	1.8×10^{-4}	22	100
EPI	180	0.003	1.7×10^{-5}	15	70

^a Anthracyclines were used 10–500 μM , and secondary alcohol metabolites were measured at 4 h.

^b Anthracyclines were used 50 μM , and secondary alcohol metabolites were measured over the linear phase of the reaction (usually 30–60 min). IC_{50} indicates concentration causing 50% inhibition of DOXOL or EPIOL formation.

^c Anthracyclines were used 50 μM , and secondary alcohol metabolites were measured at 4 h.

magnitude lower than that determined for the reduction of DOX to DOXOL (Table 4). Doxorubicinol and EPIOL were measured also in the presence of tolrestat and quercetin, general inhibitors of aldo/keto or carbonyl reductases, respectively (47). Both tolrestat and quercetin diminished the formation of DOXOL and EPIOL; however, the IC_{50} values of tolrestat always proved 4–5 times lower than those of quercetin, suggesting that both DOX and EPI were metabolized primarily by aldo/keto-reductases (see Table 4). Thus, EPI formed less alcohol metabolites than DOX mainly due to its reduced catalytic specificity for cytoplasmic aldo/keto-reductases.

DISCUSSION

Several assays showed that EPI exhibited limited one-electron reduction and formation of O_2^- or H_2O_2 in the membrane fraction of human myocardial samples. Epirubicin also exhibited limited two-electron reduction and conversion to its alcohol metabolite in the soluble fraction of these samples. The experimental model was tailored to avoiding excess drug concentration and an acute/irreversible tissue damage that could have influenced the mechanisms and levels of formation of anthracycline metabolites. Accordingly, human myocardial strips did not release protein markers after anthracycline administration (see “Characterization of a Translational Model of Human Heart” under “Results”), and O_2^- -dependent inactivation of mitochondrial aconitase was reverted by cysteine and ferrous ammonium sulfate (see Table 3). Moreover, there was only a marginal diffusion and/or accumulation of O_2^- and H_2O_2 in the soluble fraction; hence, ROS and secondary alcohol metabolites could not act in concert and induce toxic changes of cytoplasmic aconitase activity (see Table 3). These settings therefore offered an opportunity to characterize the inherent capability of human heart to promote one- or two-electron reduction of DOX or EPI.

The molecular determinants of the reduced conversion of EPI to ROS were characterized also through experiments with cell-free systems or H9c2 cardiomyocytes. This approach demonstrated that EPI could not form ROS because of its protonation-sequestration in cytoplasmic acid organelles and consequent limited access to mitochondrial one-electron reductases, which converted DOX to ROS via a semiquinone intermediate. Accordingly, the vacuolar H^+ -ATPase inhibitor bafilomycin diminished the vesicular sequestration of EPI and increased its localization to mitochondria and formation of ROS (*cf.* Figs. 4–8).

How precisely the cytoplasmic organelles of cardiomyocytes sequestered EPI but not DOX remains to be established. The pK_a values of DOX and EPI are very similar (8.34 *versus* 8.08) (48) and would anticipate a complete protonation of either anthracycline in the acidic environment of lysosomes, endosomes, or vesicles of the *trans*-Golgi network (pH \approx

5, ~ 6.5 , or ~ 6 , respectively) (40). Tentative explanations can be put forward by considering that molecules with similar pK_a values may exhibit different lipophilicity, with the more lipophilic molecule showing an improved binding to organellar membranes and a higher propensity to form aggregates in the vesicles (49). This might very well be the case of EPI, which exhibits higher lipophilicity than DOX when assessed by octanol-water partitioning (50). Re-examination of the vacuoles of cardiomyocytes sequentially exposed to bafilomycin and anthracyclines lent support to this possibility. In fact, these vacuoles always contained minor residues of EPI but not of DOX, as if EPI were more effective than DOX at diffusing into the vacuoles and forming aggregates therein (*cf.* Fig. 7, *insets A and B*). In the presence of an active vacuolar H^+ -ATPase, one such mechanism would increase the amount of EPI liable to protonation and would generate a driving force for the diffusion and sequestration of more and more EPI inside the vesicles.

Information obtained with H9c2 cardiomyocytes was successfully translated into experiments where bafilomycin increased DCF-detectable H_2O_2 formation and O_2^- -dependent inactivation of mitochondrial aconitase also in human myocardial strips exposed to EPI (*cf.* Fig. 9, *A and B*, and Table 3). These findings, and the lack of effect of bafilomycin on DOX-dependent H_2O_2 formation or aconitase inactivation, strongly suggest that a protonation-sequestration mechanism would selectively limit the reductive conversion of EPI to ROS also in human myocardium.

Anthracycline protonation-sequestration was described previously in cancer cells and was suggested to represent a cause for ineffective drug therapy under defined conditions. The available evidence shows that drug-naive tumor cells usually exhibit a defective acidification of cytoplasmic organelles, and consequently fail to sequester anthracyclines and weakly basic drugs in general (40, 51). Acquisition of the multidrug resistance phenotype is accompanied by re-acidification of cytoplasmic organelles and sequestration of anthracyclines away from the nucleus and topoisomerase II; however, the vesicular apparatus of these cells exhibit changes that diminish the importance of lipophilicity and the probability for a selective sequestration of EPI (*e.g.* expansion and clusterization of lysosomes, altered lipid composition of organellar membranes, and lysosomal and Golgi localization of multidrug transporter proteins that pump anthracyclines from cytoplasm into the vesicles) (39, 52–54). In keeping with these notions, both DOX and EPI underwent vesicular sequestration and lost their activity in resistant cells (41).

In previous studies we reported that EPI formed less alcohol metabolite than DOX under limited conditions in cell-free systems (55, 56). Here we showed that EPI formed less alcohol metabolite than DOX also in the cytoplasmic milieu of a translational model of human heart (see Fig. 10). The impaired conversion of EPI to EPIOL was not attributable to vesicular sequestration and consequent reduced availability to cytoplasmic two-electron reductases like aldo/keto-reductases or carbonyl reductases. Direct measurements of anthracycline levels in bafilomycin-treated human myocardium showed that the protonation-sequestration mechanism actually served a driving force for the transit and retention of EPI in cytoplasm prior to its vesicular sequestration or binding to other membrane compartments (see “Epirubicin Forms Less Alcohol Metabolite than DOX in Human Myocardium” under “Results”). Similar conclusions were reached in previous studies of the cellular trafficking of model molecules exhibiting high lipophilicity and pK_a values (57). Experiments with highly purified cytoplasmic fractions of human myocardium offer direct evidence that the formation of EPIOL is limited by a reduced catalytic specificity of EPI for cytoplasmic aldo/keto-reductases, resulting in an impaired two-electron addition to the side chain carbonyl group (see Table 4).

Our results now offer molecular correlates to recapitulate the therapeutic

tic index of EPI in a mechanistic framework. On the one hand, vesicular sequestration and limited specificity for cytoplasmic aldo/keto-reductases limit an intramyocardial conversion of EPI to ROS and EPIOL, which may be important culprits of cardiotoxicity. On the other hand, EPI would not undergo more protonation-sequestration than DOX in cancer cells, nor would an impaired formation of EPIOL diminish the antitumor activity of EPI (1). Epirubicin therefore shows the requisites for inducing less toxicity in cardiac cells while not losing its activity in tumor cells. This formally explains how EPI causes cardiomyopathy and congestive heart failure at doses higher than equiactive to DOX.

Currently, the lower dose-related cardiotoxicity of EPI allows for administration of more cycles of EPI than DOX before reaching a limiting cumulative cardiotoxic dose (3). Present evidence for a reduced intramyocardial conversion of EPI to ROS and secondary alcohol metabolite rationalizes this procedure beyond the glucuronidation/elimination mechanism and anticipates other important molecular readouts. One point of consideration pertains to the risk-benefit ratio of combining DOX with drugs, like the tubulin-active paclitaxel or the anti-HER2/neu antibody trastuzumab, that improve tumor response but also aggravate cardiotoxicity by increasing DOXOL formation through allosteric mechanisms (22) or by down-regulating survival pathways against ROS (58). Defective conversion to ROS and secondary alcohol metabolite should render EPI a much better partner than DOX for these drugs. Finally, the observations reported in this study highlight the protonation/sequestration mechanism and an impaired efficiency of two-electron addition as potential mechanistic templates in the search and screening of analogues that retain antitumor activity but induce less cardiotoxicity.

REFERENCES

- Minotti, G., Menna, P., Salvatorelli, E., Cairo, G., and Gianni, L. (2004) *Pharmacol. Rev.* **56**, 185–229
- Innocenti, F., Iyer, L., Ramirez, J., Green, M. D., and Ratain, M. J. (2001) *Drug Metab. Dispos.* **29**, 686–692
- Bonadonna, G., Gianni, L., Santoro, A., Bonfante, V., Bidoli, P., Casali, P., Demicheli, R., and Valagussa, P. (1993) *Ann. Oncol.* **4**, 359–369
- Ewer, M. S., and Benjamin, R. S. (2000) in *Cancer Medicine* (Holland, J., and Frei, E., eds) 5th Ed., pp. 2324–2339, B. C. Decker, Philadelphia
- Doroshov, J. H. (1995) in *Anthracycline Antibiotics: New Analogues, Methods of Delivery, and Mechanisms of Action* (Priebe, W., ed) pp. 259–267, American Chemical Society, Washington, D. C.
- Singal, P. K., Li, T., Kumar, D., Danelisen, I., and Iliskovic, N. (2000) *Mol. Cell. Biochem.* **207**, 77–85
- Kotamraju, S., Kalivendi, S. V., Konorev, E., Chitambar, C. R., Joseph, J., and Kalyanaraman, B. (2004) *Methods Enzymol.* **378**, 362–382
- Gille, L., and Nohl, H. (1997) *Free Radic. Biol. Med.* **23**, 775–782
- Gambliel, H. A., Burke, B. E., Cusack, B. J., Walsh, G. M., Zhang, Y. L., Mushlin, P. S., and Olson, R. D. (2002) *Biochem. Biophys. Res. Commun.* **291**, 433–438
- Olson, R. D., Mushlin, P. S., Brenner, D. E., Fleischer, S., Cusack, B. J., Chang, B. K., and Boucek, R. J., Jr. (1988) *Proc. Natl. Acad. Sci. U. S. A.* **85**, 3585–3589
- Mushlin, P. S., Cusack, B. J., Boucek, R. J., Jr., Andrejuk, T., Li, X., and Olson, R. D. (1993) *Br. J. Pharmacol.* **110**, 975–982
- Charlier, H. A., Jr., Olson, R. D., Thornock, C. M., Mercer, W. K., Olson, D. R., Broyles, T. S., Muhlestein, D. J., Larson, C. L., Cusack, B. J., and Shadle, S. E. (2005) *Mol. Pharmacol.* **67**, 1505–1512
- Minotti, G., Recalcati, S., Mordente, A., Liberi, G., Calafiore, A. M., Mancuso, C., Preziosi, P., and Cairo, G. (1998) *FASEB J.* **12**, 541–552
- Minotti, G., Recalcati, S., Menna, P., Salvatorelli, E., Corna, G., and Cairo, G. (2004) *Methods Enzymol.* **378**, 340–361
- Corna, G., Santambrogio, P., Minotti, G., and Cairo, G. (2004) *J. Biol. Chem.* **279**, 13738–13745
- Olson, L. E., Bedja, D., Alvey, S. J., Cardounel, A. J., Gabrielson, K. L., and Reeves, R. H. (2003) *Cancer Res.* **63**, 6602–6606
- Kang, Y. J., Sun, X., Chen, Y., and Zhou, Z. (2002) *Chem. Res. Toxicol.* **15**, 1–6
- Gewirtz, D. A. (1999) *Biochem. Pharmacol.* **57**, 727–741
- Maessen, P. A., Mross, K. B., Pinedo, H. M., and van der Vijgh, W. J. (1987) *Cancer Chemother. Pharmacol.* **20**, 85–87
- Oppermann, U. C., Maser, E., Mangoura, S. A., and Netter, K. J. (1991) *Biochem. Pharmacol.* **42**, 189–195
- LeBel, C. P., Ischiropoulos, H., and Bondy, S. C. (1992) *Chem. Res. Toxicol.* **378**, 227–231
- Minotti, G., Saponiero, A., Licata, S., Menna, P., Calafiore, A. M., Teodori, G., and Gianni, L. (2001) *Clin. Cancer Res.* **7**, 1511–1515
- Pantopoulos, K., Mueller, S., Atzberger, A., Ansoerge, W., Stremmel, W., and Hentze, M. W. (1997) *J. Biol. Chem.* **272**, 9802–9808
- Wagner, B. A., Evig, C. B., Reszka, K. J., Buettner, G. R., and Burns, C. P. (2005) *Arch. Biochem. Biophys.* **440**, 181–190
- Ramachandran, A., Moellering, D. R., Ceasar, E., Shiva, S., Xu, J., and Darley-Usmar, V. (2002) *Proc. Natl. Acad. Sci. U. S. A.* **99**, 6643–6648
- Manders, E. E. M., Verbeek, F. J., and Aten, J. A. (1993) *J. Microsc. (Oxf.)* **169**, 375–382
- Gianni, L., Viganò, L., Locatelli, A., Capri, G., Giani, A., Tarenzi, E., and Bonadonna, G. (1997) *J. Clin. Oncol.* **15**, 1906–1915
- Grasselli, G., Viganò, L., Capri, G., Locatelli, A., Tarenzi, E., Spreafico, C., Bertuzzi, A., Giani, A., Materazzo, C., Cresta, S., Perotti, A., Valagussa, P., and Gianni, L. (2001) *J. Clin. Oncol.* **19**, 2222–2231
- Finlay, G. J., and Baguley, B. C. (2000) *Cancer Chemother. Pharmacol.* **45**, 417–422
- Kalivendi, C. R., Chitambar, S. V., Joseph, J., and Kalyanaraman, B. (2002) *J. Biol. Chem.* **277**, 17179–17187
- L'Ecuyer, T., Allebban, Z., Thomas, R., and Vander Heide, R. (2004) *Am. J. Physiol.* **286**, H2057–H2064
- Kluzza, J., Marchetti, P., Gallego, M. A., Lancel, S., Fournier, C., Loyens, A., Beauvillain, J. C., and Bailly, C. (2004) *Oncogene* **23**, 7018–7030
- Kalivendi, S. V., Konorev, E. A., Cunningham, S., Vanamala, S. K., Kaji, E. H., Joseph, J., and Kalyanaraman, B. (2005) *Biochem. J.* **389**, 527–539
- Rota, C., Fann, Y. C., and Mason, R. P. (1999) *J. Biol. Chem.* **274**, 28161–28168
- Chance, B., Sies, H., and Boveris, A. (1979) *Physiol. Rev.* **59**, 527–605
- Menna, P., Salvatorelli, E., Giampietro, R., Liberi, G., Teodori, G., Calafiore, A. M., and Minotti, G. (2002) *Chem. Res. Toxicol.* **15**, 1179–1189
- Davies, K. J., and Doroshov, J. H. (1986) *J. Biol. Chem.* **261**, 3060–3067
- Gregory, J. (2002) *Handbook of Fluorescent Probes and Research Products*, Technical Note MP 07510, pp. 1–4, Molecular Probes, Eugene, OR
- Hurwitz, S. J., Terashima, M., Mizunuma, N., and Slapak, C. A. (1997) *Blood* **89**, 3745–3754
- Altan, N., Chen, Y., Schindler, M., and Simon, S. M. (1998) *J. Exp. Med.* **187**, 1583–1598
- Ouar, Z., Bens, M., Vignes, C., Paulais, M., Pringel, C., Fleury, J., Cluzeaud, F., Lacave, R., and Vandewalle, A. (2003) *Biochem. J.* **370**, 185–193
- Palmiter, R. D., Cole, T. B., and Findley, S. D. (1996) *EMBO J.* **15**, 1784–1791
- Bowman, F. J., Siebers, A., and Altendorf, K. (1988) *Proc. Natl. Acad. Sci. U. S. A.* **85**, 7972–7976
- Cubells, J. F., Rayport, S., Rajendran, G., and Sulzer, D. (1994) *J. Neurosci.* **14**, 2260–2271
- Hausladen, A., and Fridovich, I. (1994) *J. Biol. Chem.* **269**, 29405–29408
- Gardner, P. R., Raineri, I., Epstein, L. B., and White, C. W. (1995) *J. Biol. Chem.* **270**, 13399–13405
- Forrest, G. L., and Gonzalez, B. (2000) *Chem. Biol. Interact.* **129**, 21–40
- Ragunand, N., and Gillies, R. J. (2000) *Drug Resist. Updat.* **3**, 39–47
- Yokogawa, K., Ishizaki, J., Ohkuma, S., and Miyamoto, K. (2002) *Methods Find. Exp. Clin. Pharmacol.* **24**, 81–93
- Wielinga, P. R., Westerhoff, H. V., and Lankelma, J. (2000) *Eur. J. Biochem.* **267**, 649–657
- Schindler, M., Grabski, S., Hoff, E., and Simon, S. M. (1996) *Biochemistry* **35**, 2811–2817
- Olsson, J. M., Eriksson, L. C., and Dallner, G. (1991) *Cancer Res.* **5**, 3774–3780
- Gong, Y., Duvvuri, M., and Krise, J. P. (2003) *J. Biol. Chem.* **278**, 50234–50239
- Rajagopal, A., and Simon, S. M. (2003) *Mol. Biol. Cell* **14**, 3389–3399
- Minotti, G., Cavaliere, A. F., Mordente, A., Rossi, M., Schiavello, R., Zamparelli, R., and Possati, G. F. (1995) *J. Clin. Invest.* **95**, 1595–1605
- Minotti, G., Licata, S., Saponiero, A., Menna, P., Calafiore, A. M., Di Giammarco, G., Liberi, G., Animati, F., Cipollone, A., Manzini, S., and Maggi, C. A. (2000) *Chem. Res. Toxicol.* **13**, 1336–1341
- Siebert, G. A., Hung, D. Y., Chang, P., and Roberts, M. S. (2004) *J. Pharmacol. Exp. Ther.* **308**, 228–235
- Giraud, M.-N., Flück, M., Zuppinger, C., and Suter, T. M. (2005) *J. Appl. Physiol.* **99**, 313–322

Defective One- or Two-electron Reduction of the Anticancer Anthracycline Epirubicin in Human Heart: RELATIVE IMPORTANCE OF VESICULAR SEQUESTRATION AND IMPAIRED EFFICIENCY OF ELECTRON ADDITION

Emanuela Salvatorelli, Simone Guarnieri, Pierantonio Menna, Giovanni Liberi, Antonio M. Calafiore, Maria A. Marigliò, Alvaro Mordente, Luca Gianni and Giorgio Minotti

J. Biol. Chem. 2006, 281:10990-11001.

doi: 10.1074/jbc.M508343200 originally published online January 19, 2006

Access the most updated version of this article at doi: [10.1074/jbc.M508343200](https://doi.org/10.1074/jbc.M508343200)

Alerts:

- [When this article is cited](#)
- [When a correction for this article is posted](#)

[Click here](#) to choose from all of JBC's e-mail alerts

This article cites 55 references, 23 of which can be accessed free at <http://www.jbc.org/content/281/16/10990.full.html#ref-list-1>